Viscoelastic Influence on Wall and Baroreceptors of Rabbit Carotid Sinus (43443)

HENRY STINNETT,*[,1] THOMAS WIGGEN,[†] MARK OLSON,[‡] AND DANIEL EWERT[§]

Departments of Physiology, Computer Science,[†] and Anatomy and Cell Biology,[‡] University of North Dakota, Grand Forks, North Dakota 58202, and Department of Electrical Engineering,[§] North Dakota State University, Fargo, North Dakota 58105*

Abstract. **This study examined multifiber baroreceptor nerve activity (BNA) as a function of carotid sinus wall distension in 19 rabbits. Analysis estimated mechanical or viscoelastic properties of the sinus wall and their influence on BNA. In six sinuses, properties were altered by treatment with the enzyme protease to remove the endothelium and with nifedipine to passively relax smooth muscle. Properties were estimated from dynamic and steady state wall response to a 45 mm Hg step increase and decrease in intrasinus pressure (ISP) of 20 min. Control wall response had fast and slow (creep) portions with a viscosity increase from 1,370 N(s)/m to 17,864 N(s)/m during step-up in ISP. Wall elasticity averaged 77 N/m; which estimated the relationship of force and change in steady state response. Control BNA response also had fast and slow (resetting) portions. A BNA and wall response relationship (BNA/m) was defined as transduction-gain (T-G) with proportional and dynamic components. In the subgroup, wall creep and baroreceptor resetting were abolished by protease treatment, suggesting an endothelial mediator which influenced sinus smooth muscle. Histology data indicated enzyme damage was limited to tunica intima tissues, and nifedipine did not block Ca^{2+} channels on neural structures. By comparison of responses before and after treatments the proportional component of T-G was equated to an elastic influence (1/E), with $E = 7.5 \times 10^{-6}$ m/BNA, while the dynamic component was equated to a viscous influence (1/V), with $V = 1.53 \times 10^{-4}$ m(s)/BNA. A simple but fundamental relationship for baroreceptor-tissue linkages was estimated by BNA/m = 1/(Vs + E), a first-order transfer function.** [P.S.E.B.M. 1992, Vol 200]

It is well known that baroreceptor fiber activity results from pressure-mediated strain in surrounding sinus tissues. Yet, linkage mechanics between baroreceptors and the wall are not clear. A common observation is that with a large step increase in intrasinus pressure, baroreceptor multifiber activity rapidly increases as the sinus wall distends. However, if the pressure step is sustained, activity decays while the wall continues to expand or "creep." Viscoelastic relaxation, as in arteries (1), seems to explain sinus wall creep, but what causes activity decay is unclear. In the first minute, decay in activity is rapid, and this decay in an individual fiber is characterized as "adaptation" of the receptor (2). Yet, if pressure is maintained, an additional slower decay follows and is apparently due to "resetting" characteristics of the receptors, and what causes resetting is not clear. Knowledge of cause(s) is important because a consequence of *in vivo* baroreceptor resetting is that cardiovascular reflexes are altered (2–5). One hypothesis, unifying adaptation and acute resetting, is that both involve viscoelastic relaxation of coupling elements, with decreasing strain at the baroreceptor membrane (6, 7). But, the activity response decay curve does not resemble wall expansion creep. Other hypotheses for resetting propose alterations in intrinsic baroreceptor properties (8–12) or release of influential mediators during the period of altered intrasinus pressure (13, 14). In general, these hypotheses frame a controversy concerning the relative contribution that tissue-baroreceptor coupling and transduction have on fiber activity. Transduction is the conversion of receptor membrane strain into nerve fiber activity, as governed by intrinsic processes (10, 15).

Knowledge of the viscous and elastic properties of tissue-baroreceptor couplings would help us understand

[1] To whom requests for reprints should be addressed at Department of Physiology, School of Medicine, University of North Dakota, Grand Forks, ND 58202.

Received September 11, 1990. [P.S.E.B.M. 1992, Vol 200]
Accepted January 14, 1992.

0037-9727/92/2003-0359$3.00/0

how baroreceptors operate. Some studies that have examined both baroreceptor and wall responses (16–19), suggest that viscous and elastic wall elements have both a parallel and series influence on the baroreceptor, but linkage sequence is unclear. Brown *et al.* (16) examined rat aortic baroreceptor and wall responses to a "swept-frequency" sine wave intrasinus pressure input of 0.2–20 Hz. From their results, they suggested that the difference for dynamic responses of myelinated and unmyelinated baroreceptors could be due to different mechanical properties of tissues coupled to their endings. Individual carotid baroreceptor endings are coupled to smooth muscle, elastin, and collagen in the sinus adventitia (20). The anatomical evidence indicates an end to end or series link between tissue and baroreceptor. The viscoelastic properties are different for each type of tissue (1); therefore, transmitted stress would vary membrane strain at each respective ending. This alone could cause differences in activity responses between baroreceptors. However, nerve activity is also the result of intrinsic transduction processes, and these may involve exponential enzyme kinetics. The relative contribution of baroreceptor-tissue connections and intrinsic transduction processes on nerve fiber response is unknown.

The purpose of this study was to identify viscoelastic properties that relate baroreceptor and wall responses in the rabbit carotid sinus. We assumed that the viscoelastic properties of the sinus wall were basically the same as those for arterial vessels. Responses for arterial vessel segments are similar to those for systems with viscoelastic properties described by first-order or second-order differential equations with overdamped viscosity (1). Likewise, differential equations can be used to describe the relationship between baroreceptor responses and wall events to yield insight on tissue-receptor connections. Experimentally, we recorded multifiber activity and wall responses before and during 20-min step changes in intrasinus pressure. Our analysis included estimating wall viscosity from dynamic responses and elasticity from steady state responses (21). Viscoelastic influences at tissue-receptor connections were estimated by considering activity a function of wall events (not pressure) and defined the relationship as transduction-gain. In some experiments, results were compared before and after use of protease and nifedipine to assess change in viscosity caused by altering smooth muscle tone. Protease was used to enzymatically inactivate the endothelium and, thus, decrease release of vasoactive substance from endothelial cells during changes in intrasinus pressure (22, 23). Nifedipine was used to relax smooth muscle after protease treatment of each sinus. Treatment effects were examined on tissue sections prepared for transmission electron microscopy. Results were also used to estimate arrangement of viscoelastic properties that influenced baroreceptors.

Materials and Methods

Experimental Preparation. Each rabbit was anesthetized with 30 mg/kg of sodium pentobarbital (Veterinary Laboratories Ltd., Inc.) via an ear vein. Anesthesia was supplemented via a cannulated femoral vein. The femoral artery was also cannulated to record (Grass 7 Recorder) blood pressure (Statham P23Ac Transducer) and heart rate (Grass EKG/Tachograph) and to provide samples for blood gas analysis (IL 213; Instrument Laboratories). Through a midline cervical incision, the trachea was cannulated, the right preganglionic sympathetic nerve was cut (to remove central nervous system influences), and right carotid sinus was isolated vascularly using modifications of a technique described previously (24). Intrasinus perfusion and pressure levels were regulated via a system containing pressure bottles, valves, and lines connected to the vascularly isolated common carotid. The pressure in one bottle was held at 25 mm Hg, while pressure in the other was varied between 25 and 100 mm Hg. These bottles were connected by a three-way valve to the infusion line. The infusion line contained an adjustable-clamp flow resistor at about 10 cm above the inflow cannula. The resistor was adjusted to provide critically damped step inputs in pressure. Critically damped inputs were used to eliminate under- or overdamped pressure influences on the sinus wall and activity responses. The time constant for this system averaged 0.0625 sec (range, 0.060–0.065 sec) for step-up and step-down procedures between 25 and 70 mm Hg (n = 8). The infusion solution was Ringer's, modified for use in mammals, with a composition of (mM in parenthesis): NaCl (138), KCl (3.7), $NaHCO_3$ (12), $MgSO_4$ (1.3), $CaCl_2$ (1.8), NaH_2PO_4 (0.4), dextrose (5.6), and 5 g/liters of dextran (mol wt 63,200, Sigma Chemical Co.) Solution pH was adjusted to 7.4 ± 0.02 while pO_2 exceeded 130 mm Hg and pCO_2 ranged between 24 and 30 mm Hg. The system's outflow line was connected to the external carotid, at which point intrasinus pressure (ISP) was monitored (Statham P23Ac) and recorded on magnetic tape (Tandberg model 100-1) and a Grass 7 recorder. Recordings were made during conditions of no flow in a sinus.

Nerve Recordings. The carotid sinus baroreceptor afferent nerve was located and cut near its junction with the glossopharyngeal (IX cranial) nerve and prepared for recording multifiber nerve activity. Multifiber recordings were obtained using a platinum unipolar electrode (18). Recordings of background "noise" were made before and after activity recordings. Signals were amplified (model 7P511 Grass Amplifier) and stored on magnetic tape. Nerve activity and background noise were both full-wave rectified and integrated (Grass In-

tegrator model 7P10E) from the magnetic tape records. Integrated background was then subtracted from nerve activity to yield net baroreceptor nerve activity (BNA). During record analysis, BNA was normalized. BNA was set to 100% when ISP had been at 70 mm Hg for 20 min. All other activity of the nerve was expressed relative to this value as a percentage (%BNA). Integration of activity is the recommended method for quantifying multifiber responses since it minimizes error involved with occlusive summation of individual fiber activity (25). Multifiber preparations have been found to reset in rat aortic (12), rabbit (4), and dog carotid sinus (9) preparations. For this study, integrated multifiber activity was believed more appropriate to measure than single fiber activity. We believed multifiber responses included summation of mechanical influences at the baroreceptors, similar to summation of the viscoelastic influences on wall responses.

Wall Dimension and Mass Measurements. An ocular micrometer technique and manual recording of dimension were used. Two small black threads (10-0 Ethilon, Ethicon, Inc.) of approximately 0.5 mm in length were placed parallel to one another (1.5–3.5 mm apart), one on the wall of the common carotid above the sinus junction and one on the sinus side wall. The ends were spot glued (<0.01 mm^2/spot) with Nexaband (Cyanoacrylate; Bio Nexus, Inc.). We assumed negligible elastic constraint near glue spots since their summed area (0.04 mm^2) represented less than 5% of that for the sinus side (average of 4 mm^2). The distance or dimension between threads was measured with the ocular micrometer (Crosshair/Scale Micrometer; Leeds Division of Jewelmont) at fixed focal length and magnification using a Stereo Zoom microscope (AO 570; American Optical). Resolution exceeded 0.015 mm at the sinus wall. Additional measurements of dimension were made using a caliper micrometer when ISP was conditioned at 25 mm Hg (for 20 min). At the end of experimental procedures, and following fixation for histology in a subgroup, each sinus was excised and blotted and the wet weight was determined as an estimate of mass. Use of the mass estimate will be presented in discussion on viscosity damping.

Experimental Procedures

To estimate viscoelastic properties and property influences on baroreceptors, dynamic and steady state sinus wall and multifiber responses were recorded and analyzed using the methods of Beachley and Harrison (21). Following an ISP conditioning period (ISP = 25 mm Hg, for 20 min), sinus wall dimension and multifiber activity were measured before and during a nonpulsed, critically damped step-up (25 to 70 mm Hg) and subsequent step-down (70 to 25 mm Hg) in ISP. Step duration was 20 min and measurements were made at 8–12 sec, 30 sec, and then at minute intervals. Analysis was based on viscous and elastic properties of systems described by first-order or second-order differential equations (Appendix I) and detailed in a a later section.

Sinus Treatments with Protease and Nifedipine. To determine the influence of smooth muscle on wall viscoelastic properties, responses to single-step ISP procedures were measured before and after protease and nifedipine treatment. Protease was used before nifedipine to enzymatically remove or inactivate the endothelium and thus reduce the potential for pressure/flow-activated endothelial cell release of vasoactive substances (22, 23, 26, 27). Ten sinuses were perfused, at ISP = 25 mm Hg, with a protease-Ringer solution. This solution contained 0.1 mg of protease (P5147, 5.5 units/mg; Sigma) per 100 ml. Each sinus was perfused at 38°C for 15 min, followed by a flush with fresh 38°C Ringer solution. After a conditioning period (ISP = 25 mm Hg), both procedures were repeated. Four of these sinuses were prepared for histological analysis. Other methods for disruption of the endothelium, i.e., balloon catheter, glass rod, or air bubbles (28), were possible, but were considered too harsh for the rabbit carotid sinus. The remaining six sinuses were perfused at 38°C with 3×10^{-7} *M* nifedipine (N7634; Sigma) in Ringer solution at ISP = 25 mm Hg. Following an ISP conditioning period (ISP = 25 mm Hg), ISP step procedures were repeated with nifedipine in the sinus. Statistical analyses focused on the pre- and posttreatment data from the subgroup of six sinuses treated with protease and nifedipine. Histological comparisons included results from this group and some from preliminary studies (29, 30). Nifedipine is a specific Ca^{2+} slow channel (voltage-dependent) blocker and, in smooth muscle, it interrupts Ca^{2+} influx and Ca^{2+}-initiated cross bridge formation and results in depressed stress maintenance (31, 32). Heesch *et al.* (14) obtained evidence that suggested a direct influence of nifedipine on the carotid baroreceptor in dog. However, Kunze *et al.* (33), using rat aortic arch nerve-adventitia preparations free of media and endothelium, found that, at concentrations below 10^{-6} *M*, nifedipine did not alter baroreceptor response. They also indicated that voltage-dependent calcium channels did not seem to be involved with baroreceptor transduction. In a preliminary study, we examined the influence of nifedipine on rabbit carotid baroreceptor nerve activity (34) and our results were similar to those of Heesch *et al.* (14). However, nifedipine influence on endothelial release of smooth muscle vasoactive factors (35) was not recognized by us at the time.

Histology. Protease damage of sinus tissues, as well as the blocking effect of nifedipine, was histologically examined using transmission electron microscopy. The methods were similar to those of Ralevic *et al.* (28) and Barman *et al.* (36). The key to the technique was the

fact that lanthanum blocks membrane Ca^{2+} receptors and is electron dense; therefore, its location can be distinguished with transmission electron microscopy. Control and protease-treated sinuses were perfused at ISP = 25 mm Hg, with Hepes buffer and then Hepes plus $LaCl_3$ (5 m*M*) for 20 min. Sinuses were then fixed by perfusion at the conditioning ISP with cold (4°C) Karnovsky's solution for 15 min, removed, blotted, weighed, osmium-stained, embedded (Epon/Araldite), and sectioned for transmission electron microscopy. Procedures for nifedipine-treated sinuses were similar, except that the Hepes buffer also contained nifedipine (3×10^{-7} *M*).

Viscoelastic Estimates and Influences from System Analysis. With a step input in intrasinus pressure, both wall dimension and multifiber baroreceptor nerve activity have dynamic responses, as transition occurs from one steady state to another. System analysis of dynamic and steady state responses to an input were used to estimate mechanical properties (21) as follows: Step-input force (N = newton) was geometrically estimated from the steady state difference between pressure and wall area (ISP = 25 mm Hg) and pressure and wall area (ISP = 70 mm Hg). This force was divided by mean steady state dimension response, expressed in meters to estimate the elastic coefficient (*K*, units of N/m; Eq. 3, Appendix I). Viscosity (C, units of N(sec)/m) was estimated from the product of the elastic coefficient multiplied by the time constant (sec) for an event of the dynamic response (Eq. 10, Appendix I). A time constant was determined from best fit of an exponential equation to values using iterative curve fit procedures (see statistical analysis).

Estimates of viscoelastic influences on baroreceptors were based on considering wall strain as input to receptors. The relationship of mean activity and wall response, at each point in time, was determined. This ratio estimated transduction or total gain and was termed total transduction-gain (units of BNA/m). It should be noted that multiplication of wall response by transduction-gain at each point yields activity equal to the BNA response; this is not the same as measured activity, because it does not include steady state activity for ISP = 25 mm Hg. Transduction-gain was analyzed for contribution from two components, consistent with the baroreceptor static and dynamic characteristics described by Franz *et al.* (17). The two components were termed proportional and dynamic. A coefficient for the proportional component was estimated from the ratio of steady state BNA and wall responses measured at 20 min. The influence of the proportional component on activity was determined as the product of wall response, at each point in time, multiplied by this coefficient. The influence on activity from the dynamic component was estimated as the difference between proportional component and total transduction-gain influences. Arrangement of viscous and elastic properties at baroreceptors was suggested by the comparing of plots of the activity product of transduction-gain and its components to those from known viscoelastic systems (21, 37).

Statistical Analyses. Values reported are means or mean differences ± SE as calculated and graphed using Quattro (Borland International, Inc.). Statistical evaluation used analysis of variance and appropriate Student's *t* test for paired or unpaired comparisons; *P*-values equal or less than 0.05 were considered statistically significant (38). A computer program for least squares exponential curve fit was written based on the mathematical methods of Scarborough (39). For iterative least squares procedures, the coefficient of determination (r^2) was used, with $r^2 > 0.9$ selected as the criteria level for correlation of equation fit to response values. Criteria for best fit were met when wall dynamic response was analyzed for fast (0–2 min) and slow (1–20 min) events. The overlap period (1–2 min) was considered a transitional phase and use of values was expected to cause a small error in time constant determination (40). Time constants were also determined for the same fast and slow events of the multifiber dynamic response. All measured values were used to determine exponential fit and the time constants for events of dynamic BNA and wall responses. Exponential fit to means was used with transduction-gain data, as noted in appropriate sections of the Results.

Results

Activity (BNA) and wall responses were distinctly different from each other during ISP single step procedures in 19 carotid sinuses (Fig. 1). With the step-up, BNA had a rapid increase that peaked within 10 sec and was followed by a nonlinear decay in activity throughout the remainder of the 20-min period (Fig. 1A). Thus, BNA responses demonstrated adaptation (0–2 min) and acute resetting (1–20 min) characteristics for a multifiber preparation. Wall responses displayed a nonlinear increase for the same period (Fig. 1B). The slow increase, from 1 to 20 min, demonstrated that sinus wall creep occurred and was similar to arterial creep (1). Following ISP step-down, mean BNA decreased to a value below that for the prior conditioning pressure (Fig. 1A). Activity then slowly increased in a nonlinear fashion toward that for steady state at ISP = 25 mm Hg (reverse resetting). Concurrent wall responses followed a pattern of nonlinear decrease and the slow portion of the response was indicative of reverse creep (Fig. 1B). Wall responses were similar to those for systems that are described by first- or second-order differential equations with overdamped viscosity (21). System analysis of these data first examined steady state and then dynamic responses to estimate viscoelastic properties and property influences on the receptors.

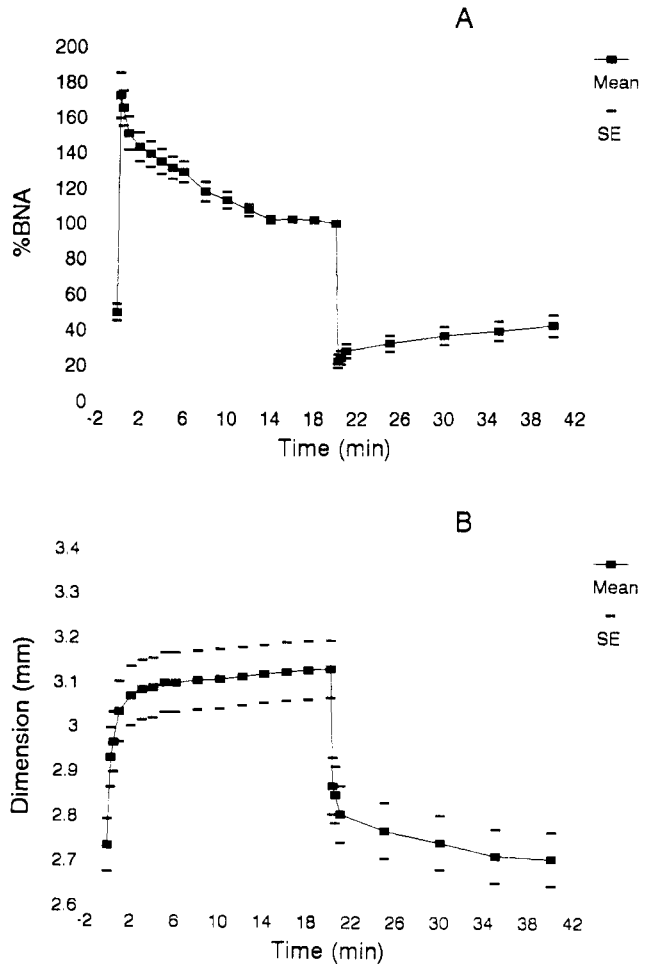

Figure 1. (A) Mean ± SE normalized multifiber baroreceptor nerve activity (%BNA) and (B) wall dimension responses to a 45-min mm Hg step-up and step-down in intrasinus pressure after a 20-min conditioning ISP of 25 mm Hg for 19 rabbit carotid sinuses, after sympathectomy. The narrowing of SE bars for (A) %BNA was due to normalization of individual values on 20-min value (100%) with ISP at 70 mm Hg. (B) Dimension responses were not normalized. Time constants from exponential regression analysis are in Table I.

Analysis Results of Steady State Responses. For both BNA and wall responses, true steady state values were approached, but not obtained, after 20 min with either step-up or -down procedures (Fig. 1). However, the mean wall response at the end of the period for the step-up in ISP was more than 98% of steady state. The percent criteria were based on the fact that four times the slow event time constant of 232 sec (Table I) did not exceed 20 min (21). This point of near steady state for responses will be clarified during analysis of data before and after enzyme and nifedipine treatments. Results here suggested that responses indicative of wall creep and multifiber baroreceptor resetting would have continued well beyond the 20 min of the pressure step. For the step change in intrasinus pressure, a tangential wall force (ΔF) was calculated as 3158 ± 411 dyne or about 0.0316 N and the mean response in steady state wall dimension (ΔDim) was 0.41 ± 0.08 mm. The wall elastic coefficient (K) was determined from $K = \Delta F/\Delta Dim$ (Eq. 3, Appendix I) and estimated as 77 N/m. This elastic coefficient represents matrix properties of all tissues; however, since responses to high intrasinus pressures (>150 mm Hg) were not examined, the major contributor was probably elastin, as will be considered in the Discussion.

The ratios of steady state wall and BNA responses were determined to obtain the coefficient for the proportional component of transduction-gain. The mean change in activity (ΔBNA) was 53.8 ± 5.2 %BNA from one steady state to the next. Note that the SE value is that for BNA at ISP = 25 mm Hg, because values at ISP = 70 mm Hg were set to 100% (Fig. 1). Also, recall that the mean steady state wall response was 0.41 mm. Thus, the steady state ratio was 131.2 BNA/mm, for a coefficient of 1.31×10^5 BNA/m for the proportional component of multifiber transduction-gain.

Analysis Results of Dynamic Responses. To characterize dynamic responses, time constants for both wall and BNA transients were determined. An initial attempt to fit a single exponential equation to all 20-min wall or BNA values yielded an $r^2 \leq 0.7$ for each data set. This did not meet criteria for best fit of the equation. Dynamic response values were then separately grouped into fast (0–2 min) and slow (1–20 min) events and each group was fit with an exponential equation. These procedures yield equations that fit with $r^2 > 0.9$. For both BNA and wall responses, slow event time constants were more than 10 times those for fast events (Table I).

Wall fast and slow event time constants (Table I) were used to estimate viscosity during each event. The coefficient for wall viscosity was calculated by multiplying the elastic coefficient by the fast event time constant (Eq. 10, Appendix I). During fast event, the step-up value was 1,370 N(sec)/m and the step-down value was 940 N(sec)/m. The reason for the difference in these values is not readily apparent, but different processes for rapid wall expansion and contraction is suggested. Recall, wall response during slow event indicated creep and reverse creep. Slow event viscosity during step-up was estimated at 17,864 N(sec)/m and at 49,280 N(sec)/m during step-down. The increase in viscosity from fast to slow event suggested the presence of a controller or feedback factor. Characteristics of this factor were examined with analysis of results before and after protease and nifedipine treatments and are presented later.

Relationship of Activity and Wall Responses. This relationship was examined by comparison of response time constants and determining multifiber transduction-gain. Time constants for BNA responses were more than double those for the wall (Table I). These results demonstrated that multifiber adaptation and resetting were preceded by fast and slow event wall responses, respectively. However, these results, involv-

Table I. Response Time Constants (τ) for Multifiber BNA, Wall Dimension, and Total, Dynamic, and Proportional Components of Transduction-Gain for 19 Rabbit Carotid Sinuses[a]

Variable	Step-up τ (sec)		Step-down τ (sec)	
	Fast event	Slow event	Fast event	Slow event
BNA	43.4 ± 5.3	544 ± 49	37.0 ± 11.5	NL
Dim	17.8 ± 2.4[b]	232 ± 14[b]	12.2 ± 1.8[b]	640 ± 53
Transduction-gain (for Fig. 2A)				
$T\text{-}G_T$	32.0	359	32.2	776
Total T-G and T-G components multiplied by dimension response (for Fig. 2B)				
$T\text{-}G_T \times$ Dim	47.2	551	44.0	NL
Components				
$T\text{-}G_D \times$ Dim	35.3	391	41.7	NL
$T\text{-}G_P \times$ Dim	16.1	238	13.7	592

[a] Analysis was of fast (0–2 min) and slow (1–20 min) events of dynamic responses to an intrasinus pressure step of 45 mm Hg. Initial ISP conditioned at 25 mm Hg for 20 min. Abbreviations: DIM, wall dimension; T-G, transduction-gain; NL, near linear regression with $\tau > 1000$ sec; T, total; D, dynamic; P, proportional. Values are mean ± SE; exponential curve fit procedures based on coefficient of determination (r^2) > 0.9. All fast event time constants were significantly less (paired t test, $P < 0.05$) than those for slow event for each variable. Regression on means was used for analysis of transduction-gain and components.
[b] Wall dimension time constants were significantly less than those for BNA.

ing the decay of activity, do not indicate whether baroreceptor activation leads or lags the wall response. The issue of lead-lag requires analysis of swept-frequency responses, which was not done in this study. Transduction-gain was calculated as the ratio of change in mean BNA activity (ΔBNA) divided by change in the mean wall dimension (ΔDim) at each point in time. Transduction-gain varied with time; it rapidly peaked and then decayed during the step increase in pressure. The reverse occurred with the step decrease in pressure (Fig. 2A). Exponential analysis was applied and $r^2 < 0.8$ for fit of a single equation to all values, while $r^2 > 0.9$ for equation fit to values for each event. Total transduction-gain time constants were less than those for BNA during a comparable event (Table I). Since transduction-gain (units of BNA/mm) estimates a transfer function, the above results indicated variability of this transfer function during dynamic response. Further insight was sought with analysis of the influence of transduction-gain and its components on multifiber activity.

Activity from Transduction-Gain Components. Total transduction-gain and the coefficient of the proportional component were each multiplied by the mean wall response at each point in time (Fig. 2B). The proportional component product was then subtracted from the total transduction-gain product in order to estimate the dynamic component influence on the activity response. For each influence, exponential equations were fit and event time constants were determined (Table I). Recall, the proportional component estimate was 131.2 BNA/mm (or 1.31×10^5 BNA/m). If baroreceptor transduction was a linear function of sinus wall distension, then gain would be composed only of a proportional component and BNA responses would be similar to those of the wall (dashed line, Fig. 2B), with essentially equal time constant values (Table I). Obviously, this is not the case, because transients occurred in BNA response. These transients represent influence of the dynamic component of transduction-gain (asterisks, Fig. 2B). We noted that while activity due to the proportional component was increasing, activity due to the dynamic component was decreasing with step-up in ISP and the reverse occurred with step-down. The rate of each component's contribution to activity summation was indicated by its respective event time constant (Table I). We interpreted these results as follows: With the step-up in ISP sustained over time, the proportional component produced increased or loading strain on the baroreceptors. At the same time, the dynamic component produced decreased or unloading strain. Other possibilities will be presented in the discussion. Processes for each component were reversed with the step-down in ISP and indicated another interesting point. During the step-down in ISP, the dynamic component seemed to contribute an "inhibitory" influence to the activity sum. To our knowledge, factors that inhibit transduction processes inside the baroreceptor have not been reported. These results would support the concept that summation of elastic- and viscous-related influences occurs at the baroreceptor membrane prior to internal processes of transduction. Additional viscoelastic influences were revealed with analysis of responses before and after protease and nifedipine treatments.

Responses before and after Protease and Nifedipine Treatments. For this subgroup of sinuses, control responses for both BNA and the wall (boxes, Fig. 3) were similar to those for the whole group (Fig. 1). Dynamic responses contained both rapid and slow events. Protease (dashed line, Fig. 3) and then nifedi-

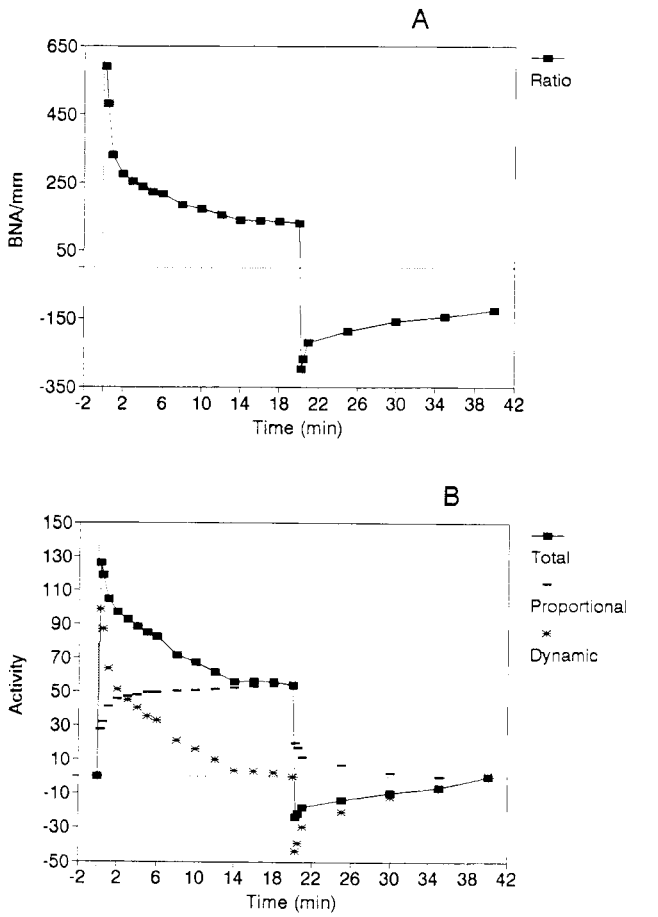

Figure 2. (A) Transduction-gain and (B) activity as a function of transduction-gain and wall distension (solid boxes) were determined for sinuses of Figure 1. (A) Transduction-gain was calculated as the ratio of mean BNA activity (ΔBNA) response divided by mean wall dimension (ΔDim) response at each point in time. For step-up in ISP, a response was the difference between the value at ISP = 25 mm Hg and the value at a given time with ISP = 70 mm Hg. For step-down in ISP, a response was the difference between the 20-min value at ISP = 70 mm Hg and the value at a given time with ISP = 25 mm Hg. (B) Influence on multifiber activity of total, dynamic, and proportional components of transduction-gain. See text for component estimate calculations. Following an intrasinus pressure step, activity due to the (B) dynamic component (asterisks) rapidly spiked and decayed toward steady state, whereas (B) activity due to the proportional component (bars) followed wall distension. Time constants from exponential regression analysis are in Table I.

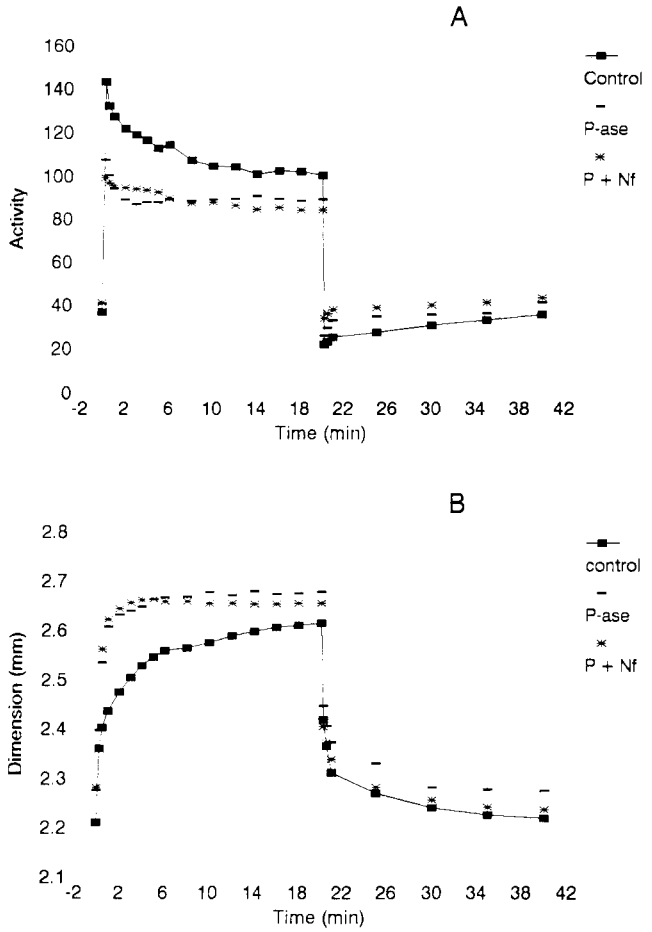

Figure 3. (A) Mean multifiber baroreceptor activity (%BNA) and (B) wall responses to the intrasinus step procedures before protease (boxes) and after (bars), and then nifedipine (asterisks) treatment in a subgroup of six sinuses of Figure 1. For clarity of responses between control and treatments, the SE values are not shown.

pine (asterisks, Fig. 3) treatments almost abolished slow event dynamic BNA and wall responses, but barely altered steady state responses. Protease treatment seemed to have the major effect, whereas subsequent treatment with nifedipine had little additional influence. After both treatments, wall steady state values were slightly increased (Fig. 3B) from the controls. However, statistical analysis indicated no significant difference among respective steady state values. Apparently, neither treatment noticeably altered the elastic properties of these sinuses and the average elastic coefficient was estimated as 82 N/m.

In controls, analysis of wall dynamic response indicated that viscosity increased from 1,535 N(sec)/m during fast event to 22,489 N(sec)/m during slow event and defined creep in this subgroup. The increase in viscosity during the step-up in ISP was abolished after the treatments. Yet, in contrast to responses during step-up, wall responses during step-down procedures were essentially unaltered by either treatment (Fig. 3B). These results indicated that reverse creep involved a process sequence different from one that would be a simple reversal of the sequence governing expansion creep. To examine this further, we subtracted control wall response from those following nifedipine treatment (Fig. 4). Following step-up in ISP, this difference rapidly peaked and then slowly decreased in a nonlinear manner. With the step-down in ISP, there was a break and departure from the slow decrease during step-up. These results suggest that the rapid rise indicated onset and effect of a factor that caused a nonlinear increase in viscosity in the controls. The slow decrease represented decay of the factor's influence. Additional characteris-

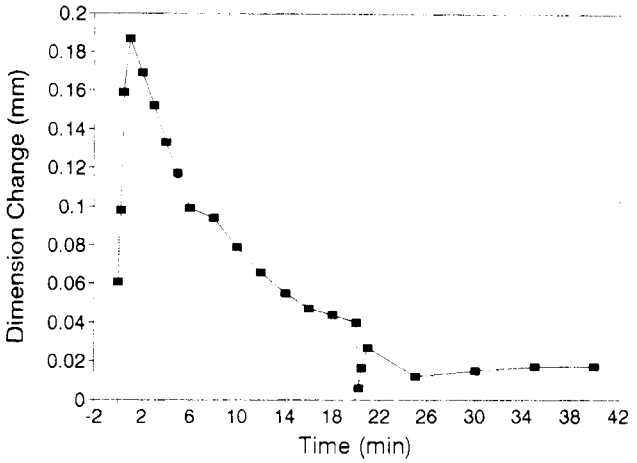

Figure 4. The presence of a controller or feedback influence on viscosity in the sub-group was evident from the net wall response difference between control and nifedipine treatment. Exponential analysis indicated an onset time constant of 33.9 sec. The curve break occurred at the step-down in intrasinus pressure. See text for further description.

tics of this factor will be examined in the Discussion section.

Dynamic BNA responses were highly reduced after protease treatment and the effect was unchanged with subsequent nifedipine treatment (Fig. 3A). These results suggest inactivation or "poisoning" of the baroreceptors by protease and perhaps nifedipine. However, this may not be the case. After either treatment, both BNA and wall responses reached steady state at 6–8 min with step-up in ISP. In contrast, neither control BNA nor wall responses had completely attained steady state after 20 min. It is likely that control BNA response would have reached the same steady state as that observed after treatments if more time had been allowed at each pressure step. However, to be consistent with prior analysis, treatment results were normalized to control results, i.e., 20 min control BNA = 100%, after protease BNA = 89 ± 12.7% and after nifedipine BNA = 85 ± 12.5% (Fig. 3A).

Transduction-Gain and Viscoelastic Influences before and after Treatments. The influence of protease and nifedipine on the relationship of BNA and wall responses was examined by analysis of the change in activity contributed by the components of transduction-gain (Fig. 5). Subgroup control results (Fig. 5A) were essentially the same as those for the whole group (Fig. 2B). Response curves for activity, due to the proportional component, following protease (Fig. 5B) and nifedipine (Fig. 5C) were similar to respective wall response curves (Fig. 3B) and similarity extended to time constant values (Table II). Steady state activity due to the proportional component seemed little altered by either treatment (Fig. 5). From mean steady state BNA and wall responses, the coefficient for the proportional component of transduction-gain for the subgroup

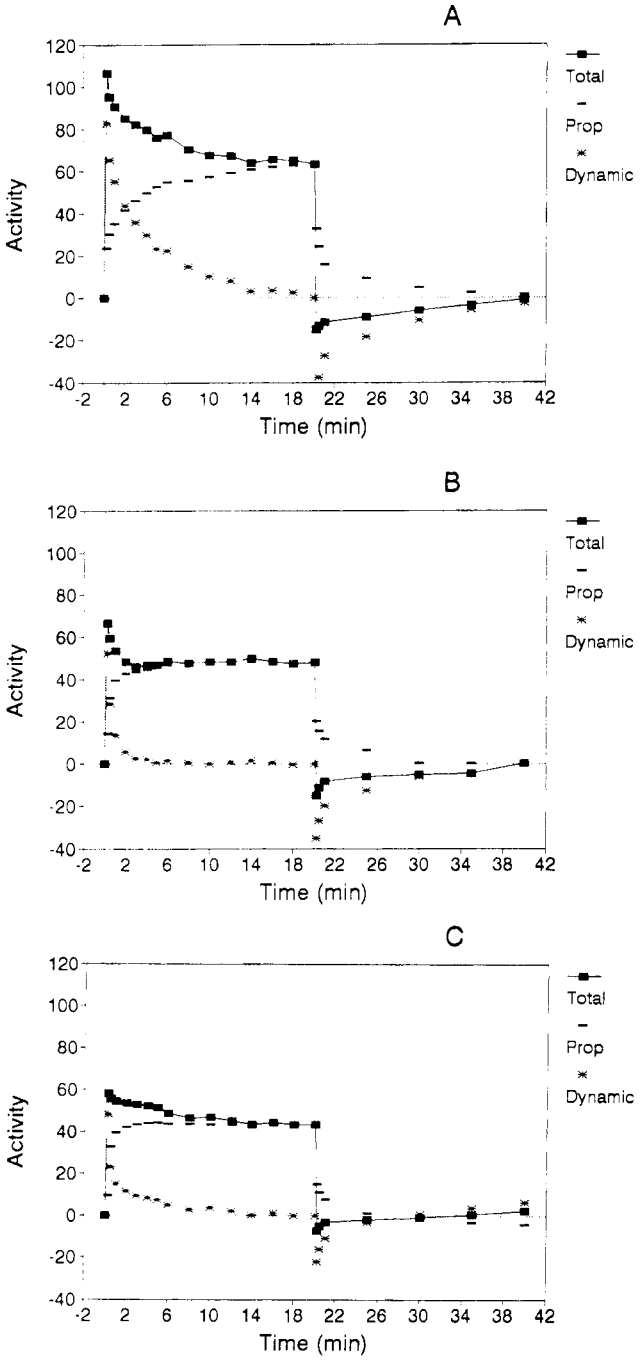

Figure 5. Multifiber baroreceptor activity as a function of total transduction-gain and wall distension (boxes), the dynamic component (asterisks), and the proportional component (bars) of transduction-gain in (A) controls and following (B) protease and (C) nifedipine treatments in the subgroup. Compared with controls, a large decrease in activity due to the dynamic, but not proportional, component resulted from protease treatment. Nifedipine had little added effect. Time constants from exponential regression analysis are in Table II.

was calculated as 1.33×10^5 BNA/m for controls, 1.37×10^5 BNA/m after protease treatment, and 1.24×10^5 BNA/m after nifedipine treatment. Since wall distension was considered input to the baroreceptors and since the proportional component of transduction-gain was based on steady state responses, we considered

Table II. Time Constants (τ) of Transduction-Gain, Proportional, and Dynamic Components of Transduction-Gain Multiplied by Wall Dimension Response for Six Rabbit Carotid Sinuses[a]

Variable	Step-up τ (sec)		Step-down τ (sec)	
	Fast event	Slow event	Fast event	Slow event
$T\text{-}G_T \times Dim$				
Control	29.8	371	51.9	NL
Protease	36.2	NL	30.1	NL
Protease, nifedipine	22.8	NL	30.7	NL
$T\text{-}G_P \times Dim$				
Control	18.7	274	19.0	452
Protease	27.7	173	13.2	363
Protease, nifedipine	28.7	48.1	12.9	328
$T\text{-}G_D \times Dim$				
Control	34.0	322	38.5	726
Protease	22.9	64.1	27.0	658
Protease, nifedipine	12.8	132(pf)	28.8	560

[a] After control recordings, sinuses were treated with protease and the nifedipine. Analysis is of fast (0–2 min) and slow (1–20 min) events of dynamic responses to a step-up and step-down in intrasinus pressure of 45 mm Hg. Values have a coefficient of determination (r^2) > 0.9. Abbreviations: T-G, transduction-gain; Dim, wall dimension; T, total; P, proportional; D, dynamic; NL, near linear regression, $\tau > 1000$ sec; pf, poor fit, $r^2 < 0.7$.

the proportional component to be reciprocally related to an elastic influence (E) at the baroreceptors (Eq. 12, Appendix I). Estimates for elastic influence during the different conditions were calculated and were 7.52×10^{-6} BNA/m for controls, 7.30×10^{-6} BNA/m after protease, and 8.06×10^{-6} BNA/m after nifedipine. Apparently, since elastic influence estimates were similar, no decrease occurred in the elastic-related influence due to the treatments.

Compared with controls (Fig. 5A), protease altered fast event activity and essentially abolished slow event activity due to the dynamic component during the step-up in ISP (Fig. 5B). Nifedipine's subsequent influence was minor (Fig. 5C). Yet, initial activity, influenced by the dynamic component, was present during fast events, ISP step-up or step-down, following both treatments (Fig. 5, B and C). From the dynamic component of transduction-gain, viscous-related influences at the baroreceptors were determined. Coefficients (V_F and V_s) for viscous-related influences were calculated by multiplying the time constant for each event (Table II) by the constant E for the elastic-related influence during a condition (Eq. 14, Appendix I). For controls $V_F = 2.55 \times 10^{-4}$ m(sec)/BNA and $V_s = 2.42 \times 10^{-3}$ m(sec)/BNA (note, $V_s = 10V_F$). After protease $V_F = 1.67 \times 10^{-4}$ m(sec)/BNA and $V_s = 4.67 \times 10^{-4}$ m(sec)/BNA, and after nifedipine $V_F = 1.02 \times 10^{-4}$ m(sec)/BNA, but V_s was not determined because of the unreliable time constant for the slow event (Table II). The loss of a viscous-related influence after both treatments suggests that a common factor was influencing wall and baroreceptor responses in the controls, and this will be examined in the Discussion.

Histology. Transmission electron microscopic examination of control tissues demonstrated penetration and deposition of lanthanum on cells in all layers of the sinus wall (Fig. 6). Layers of smooth muscle and intervening elastic lamina numbered between nine and 13 for the tunica media of these sinuses. As indicated in Materials and Methods, lanthanum ions displace those of calcium with an apparent block of calcium channels on living membranes (36). Deposition of lanthanum will occur unless the channel is blocked previously by a specific agent that has a higher affinity for the given channel. Lanthanum deposition on media smooth muscle within sinuses treated with only nifedipine (Fig. 7C) was decreased as compared with the untreated control (Fig. 6C). Not all lanthanum deposition was blocked, because there are calcium channels other than slow ones. Also, as compared with control (Fig. 6B), lanthanum deposition on the endothelial cell membrane was decreased by pretreatment with nifedipine (Fig. 7B), and these results are consistent with the presence of slow Ca^{2+} channels on endothelial cells as well as smooth muscle. Nifedipine pretreatment did not alter lanthanum deposition on nervous tissue within the sinus adventitia (Fig. 7D) as compared with controls (Fig. 6D). These results indicated a lack of slow Ca^{2+} channels on Schwann cell and neuron, and nifedipine, at 3×10^{-7} *M*, had little direct effect on the baroreceptors. These results are consistent with those of Kunze *et al.* (33).

Enzymatic damage resulted in the loss of much of the endothelium. Damage was exemplified by indiscriminate deposition of lanthanum on cell membrane debris, even when the sinus was pretreated with nifedipine (Fig. 8B). This observation provided a method for analysis of tissues damaged by protease. That is, when protease damaged a cell membrane, then nifedipine could not restrict lanthanum deposition. The abluminal side of the intima-media elastin border showed little damage and, in general, was intact. At fenestrations of the elastin border, media smooth muscle occasionally showed lanthanum deposits, indicating membrane damage. These fenestrations were not caused by protease and are where contact normally occurs between endothelium and media smooth muscle. Compared with controls, lanthanum deposition was decreased on smooth muscle membranes in deep media layers and indicated that enzyme damage did not penetrate to these tissues (Fig. 8C). No damage was observed at the media-adventitia interface or with structures within the tunica adventitia (Fig. 8D).

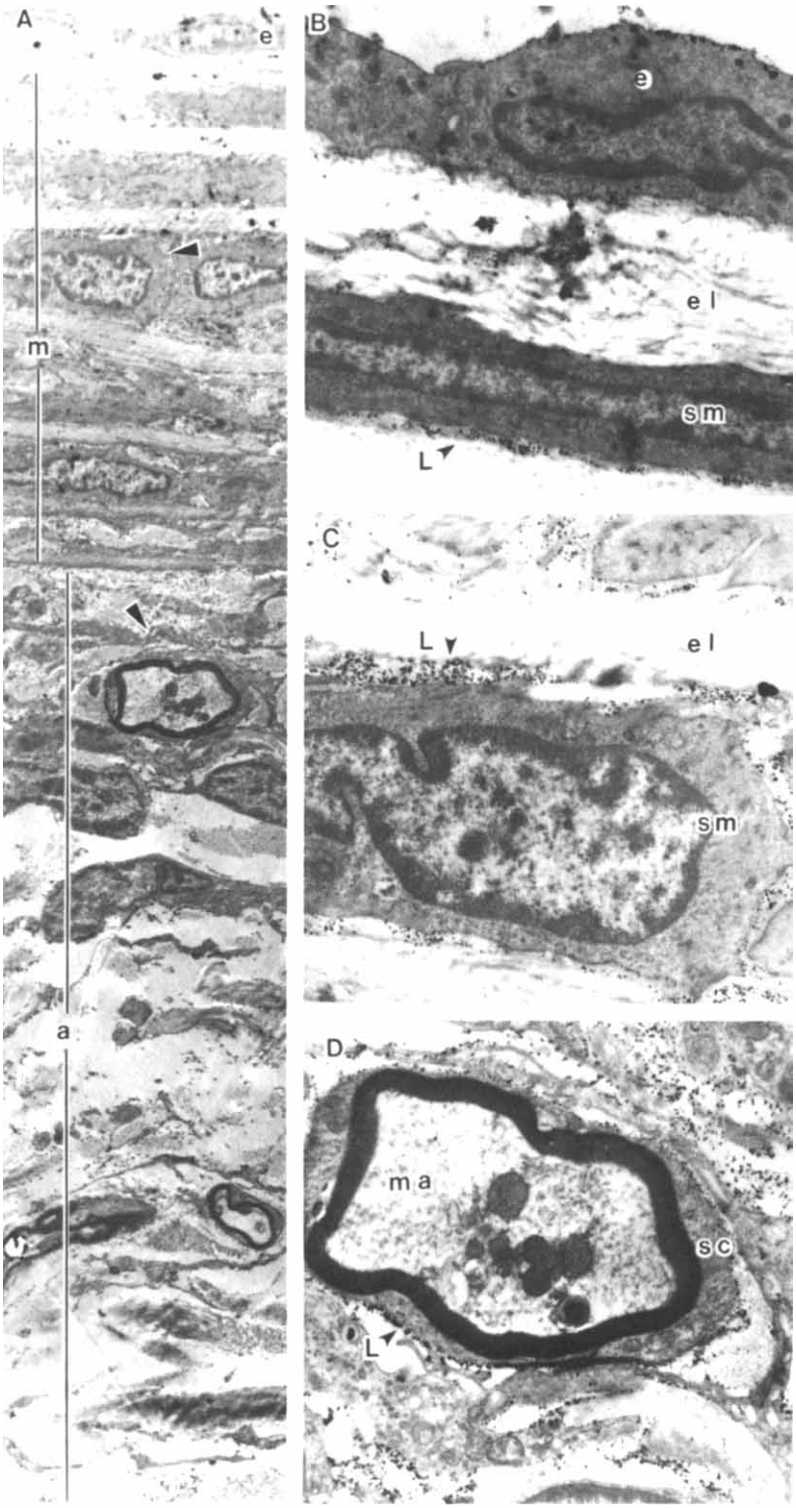

Figure 6. Photomicrographs of (A) tissue layers and (B–D) cell membranes within layers in a control rabbit carotid sinus. To visualize lanthanum deposition, tissues were not counterstained with lead or uranyl acetate here and in Figures 7 and 8. About 0.22 mm of a radial axis section, from intima to tunica adventitia, is shown in (A) (×1000). (A) Arrows are aids to location of tissues shown in (B–D) (×8000). Abbreviations: a, tunica adventitia; e, endothelial cell of intima; el, elastin; L, examples of lanthanum deposits as indicated by black dots; m, tunica media; ma, myelinated axon; sc, Schwann cell; sm, smooth muscle. Note that ubiquitous lanthanum deposition was found adjacent to plasma membranes on (A) endothelial, (A, B) smooth muscle, and (D) Schwann cell surrounding myelin (dark band) of axon (D).

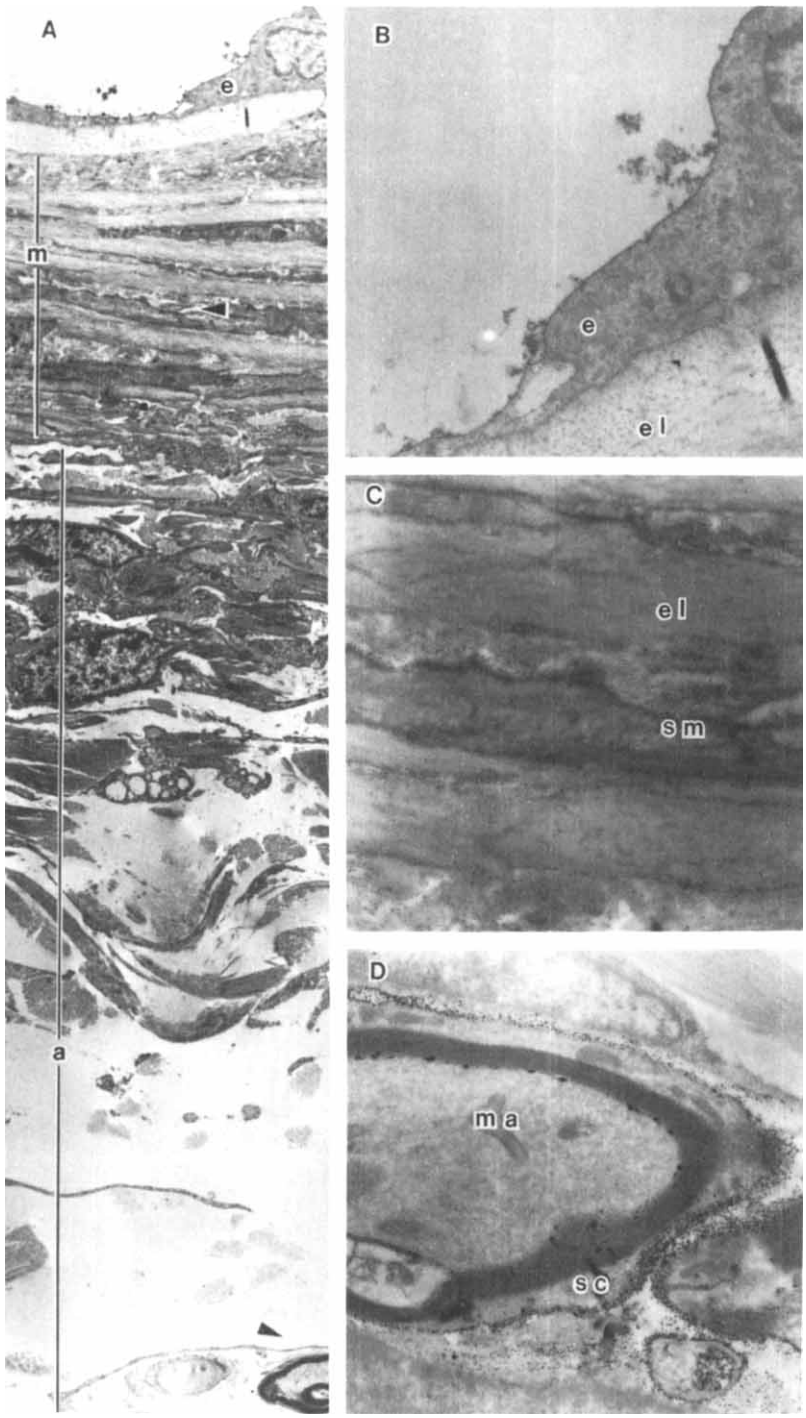

Figure 7. Photomicrographs of (A) tissue layers and (B–D) cell membranes within layers in an example of a rabbit carotid sinus treated only with nifedipine. In comparison to respective control structures (Fig. 6), lanthanum deposition was absent or reduced at membranes of both (B) endothelial and (C) smooth muscle cells, both of which contain Ca^{2+} slow channels blocked by nifedipine. Lanthanum deposition at (D) neuronal structures, which apparently do not contain Ca^{2+} slow channels, was the same as controls. Note penetration of lanthanum through myelin of the (D) axon. Sample size, magnifications, and abbreviations are the same as in Figure 6.

Discussion

Validity of Wall Property Estimates. This study estimated viscous and elastic properties of carotid sinus and the influence of these properties on sinus wall creep and baroreceptor adaptation and resetting. Validity of property estimates was sought by comparison with other determinants. Recall, a key factor for estimating wall viscosity was the elastic coefficient of 77 N/m. This elastic coefficient can be expressed as a Young's elastic modulus of 21 N/cm^2, when wall thickness (histologically estimated) was considered for these sinuses. Dobrin (1) indicated a range for the elastic

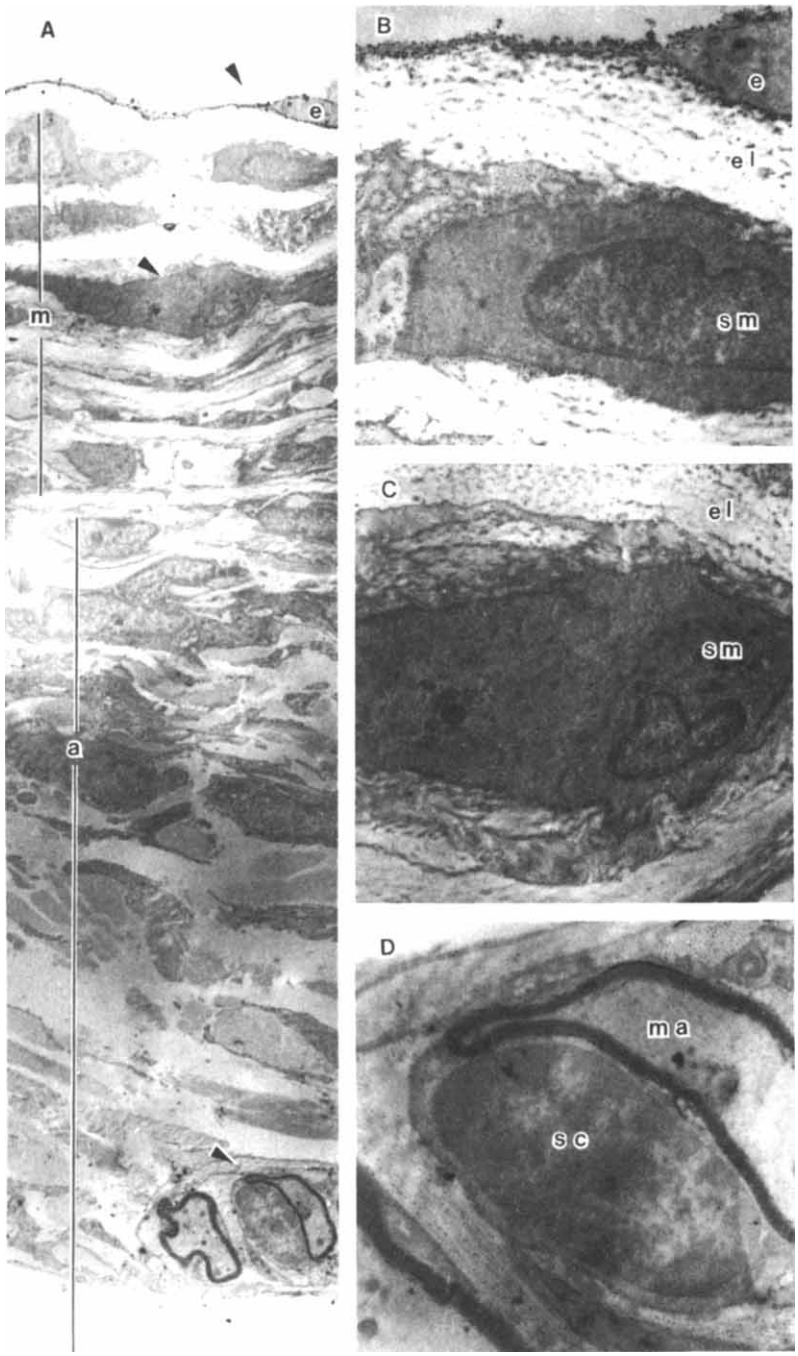

Figure 8. Photomicrograph of (A) tissue layers and (B–D) cell membranes within the layers of an example of a protease and then nifedipine-treated rabbit carotid sinus. (B) Lanthanum deposition occurred on endothelial cell debris and was indicative of enzyme damage. Lanthanum deposition was reduced at (B, C) smooth muscle membranes in the presence of nifedipine, indicating no observable protease damage beyond the external elastic lamina. Lanthanum deposition on (D) neuronal structures was unaltered by protease and essentially the same as that found in control (Fig. 6D) and sinus treated only with nifedipine (Fig. 7D). Sample size, magnifications, and abbreviations are the same as in Figure 6.

modulus of elastin, as found by various investigators, to be 15–41 N/cm^2 for aortic wall preparations. In this study, it is unlikely that wall response included contribution of a collagen influence, since the elastic modulus for collagen is 1000 times that for elastin (1). Also, following both treatments in the subgroup of sinuses, we recorded wall responses to 15 mm Hg stair-step increases and decreases in intrasinus pressure over the range of 25–100 mm Hg with each step held for 60 to 70 sec (unpublished data). Wall responses linearly increased and decreased without offset and these results demonstrated linear elastic properties of the sinus wall. Apparently, our estimate of an elastic coefficient seems to be a reasonable value and reflects a major influence from wall elastin.

Control sinus wall viscosity (C_f) averaged 1,155

N(sec)/m during fast event of the dynamic response. Because sinuses are "real systems," they have mass; therefore, this mean viscosity represents an initial high damping for the carotid sinus wall. Damping was determined from the ratio of C_f:C_c and was 14,713 (Eq. 22, Appendix I). The "critically-damped viscosity" (C_c) was 0.0785 N(sec)/m and determined from $C_c = 2(MK)^{1/2}$ with M = average sinus mass of 2×10^{-5} kg (Eq. 21, Appendix I). However, the value of C_c may be low because mean sinus wet weight (20.2 ± 1.2 mg) may underestimate mass. Other mass components could be involved and may include intraluminal fluid mass and inertia. What constitutes sinus mass during dynamic response is still unclear and might best be estimated from analysis of wall response to swept-frequency pressure input (21). Thus, the fast event viscosity estimate may be imprecise, as it was a first-order approximation for a system with mass. Yet, the error may not be critical. We have computer tested the first-order estimates of viscosity in a second-order differential model and found close simulation of mean wall response during fast event (41, 42). Results of high damping for the rabbit carotid sinus wall are consistent with the damped response found for the rat aorta (16).

Feedback Influence. An important finding of this study was the evidence for a controller or feedback factor on wall viscosity during dynamic response in the subgroup controls (Fig. 4). The data were examined to characterize the nonlinear influence. The control mean steady state wall response of 0.39 mm (3.9×10^{-4} m) was considered stimulus (y). This was divided by the fast to slow event viscosity increase of 20,955 N(sec)/m to estimate a linear coefficient (W) of 1.78×10^{-8} m^2/N(sec). Using exponential equation fit to values for the first minute (Fig. 4) yielded an onset time constant of 33.9 sec ($r^2 = 0.99$). The time constant was multiplied by W to calculate a nonlinear coefficient (Z) of 6.02×10^{-7} m^2/N. The implied differential equation for the influence of wall distension (y) on viscosity (C) was:

$$Z(dC/dt) + WC = y \qquad \text{[Eq. 1]}$$

We interpret these data to suggest that, in control sinuses, with the step change in intrasinus pressure, a controller or feedback process was "turned on" and caused a nonlinear (or pulsed) change in viscosity. Change in viscosity was a function of the direction and amplitude of wall distension. It is unlikely that the effect was controller influenced, since this is one in which the strain sensor and mechanism for response would be located in the same tissue (i.e., smooth muscle). If a controller was present, then wall response would have been little altered by protease treatment. Yet, wall slow event dynamic response was essentially abolished after protease (Fig. 3B) and histological data indicated protease damage was limited to the endothelium. Apparently, the effect involved feedback and the onset time constant would likely include components for mediator release and mediator-influenced vasoconstriction. Presumably, the strain sensor was located in endothelial cells, but involvement of sympathetic fiber endings cannot be excluded. While feedback kinetics were apparently first order, no attempt was made to identify the mediator(s). However, results are consistent with release of constrictor factor(s) from endothelial cells during conditions of increased strain (22, 23). The feedback first-order differential equation is similar to one proposed by Srinivasan and Nudelman (43); however, the elastic coefficient was nonlinear in their equation. We suggest that nonlinear viscosity may be a physiological explanation as important as nonlinear elasticity. While we proposed that viscosity was a function of the amplitude of distension, it is also possible that feedback may have been triggered by the rate of wall distension or by both.

Estimates of Viscoelastic Influences at the Baroreceptors. A key approach in this study was to consider nerve activity as a function of wall distension and not of the intrasinus pressure input (Eqs. 11–14, Appendix I). When activity was considered a function of the pressure input, the derived transfer functions were complex (15–17, 42–45). The complexity involves interaction of at least two systems, i.e., wall response to pressure or force input (System 1) and baroreceptor response to transmitted wall strain (System 2). If properties for the wall are not known, there is essentially little ability to resolve the viscoelastic properties for tissue-baroreceptor links from the activity-pressure transfer function. We circumvented this problem by relating activity to wall response over time and termed this relationship transduction-gain. Transduction-gain was considered to be composed of dynamic and proportional components. Methods of system analysis were used to determine each component, but the conceptual basis for these components was the static and dynamic response characteristics for baroreceptors as described by Franz *et al.* (17).

Examination of the components of transduction-gain led to estimates of elastic- and viscous-related influences at the baroreceptors. From the proportional component of transduction-gain, for the subgroup controls, an elastic-related influence ($E = 7.52 \times 10^{-6}$ m/BNA) at the baroreceptors was determined. Because this influence was determined from steady state wall and BNA responses, this indicated that the extrinsic elastic influence directly governed steady state strain at the membrane of the baroreceptors. Also, for baroreceptors exhibiting steady state activity, these data indicated that intrinsic processes of transduction seemed to involve zero order enzyme kinetics. From the dynamic component of transduction-gain, coefficients of viscous related influences (V_F and V_S) were calculated for fast

and slow events before and after the treatments. In controls, we considered V_S to represent essentially an extrinsic viscous influence from tissues attached to the baroreceptors, because V_S was not present after either treatment. Yet, activity due to the influence of the dynamic component of transduction-gain was still present after nifedipine treatment (Fig. 5C) and related to a V_F of 1.02×10^{-4} m(sec)/BNA. Apparently, this V_F involved processes of transduction not removed by nifedipine (or protease) treatment. These processes may involve a mass influence at the baroreceptor, or first-order enzyme kinetics of intrinsic transduction. The fact that a peaking frequency has been found for rat myelinated aortic baroreceptors (16) is evidence for a mass influence. We speculate that baroreceptor adaptation may be the transient of an apparent mass influence and acute resetting indicative of transients for viscous influences at the baroreceptor.

We propose that E and V are property-related estimates for baroreceptor-tissue links. The linkage relationship can be expressed by the activity-wall transfer function:

$$\text{BNA/m} = 1/(V_S + E) \qquad \text{[Eq. 2]}$$

where $s = \text{d/dt}$. Note, the units of this transfer function are the same as transduction-gain (Fig. 2). We realize that this transfer function is simple. It does not contain a nonlinear viscous term representing feedback. Feedback may involve attached smooth muscle, as suggested by results of this study, or a direct influence of mediator(s) on baroreceptors. The transfer function does not contain a second-order term representing an apparent-mass influence, and this influence needs to be characterized. Yet, we believe this transfer function represents a fundamental mechanical relationship governing events at tissue-baroreceptor junctions. Certainly, any formulation that would attempt to describe all interactions at the baroreceptor would have to consider feedback and mass influences.

Location of Viscous and Elastic Properties. The configuration of the activity response curve, was not like that of the wall (Fig. 1), but it was similar to movement of a point within a mechanical model (38). In the model, this point is positioned between elastic and viscous elements (elastic-:-viscous). When a step force is applied to the viscous element and the elastic element is attached to base, the point response over time simulates activity due to the dynamic component of transduction-gain (Figs. 2 and 5). Reversing the viscous and elastic elements does *not* yield the same results. If the viscous element is replaced by a second elastic element, the point response simulates activity due to the proportional component of transduction-gain (Figs. 2 and 5). When the point was modeled with mass and reduced viscosity (46), the response simulated results indicative of an apparent mass influence, as found here (Fig. 5, B and C) and, as we interpret, in the results of others (16, 47). In modeling studies (41, 46), we considered the first elastic element (attached to base) to represent elasticity of the tethered baroreceptor fiber. The viscous and second elastic elements represent properties for tissue links between the receptor membrane and other (parallel-linked) surrounding tissues. A more detailed discussion of wall and baroreceptor models and the use of models for interpreting experimental data has been presented (45).

Concluding Remarks

The operation of baroreceptors within the sinus wall is complex because of interactive processes. Franz *et al.* (17) stated that "the differential equations describing the (baroreceptor activity) response to small pressure variations must be of third- or at least second-order." From the results of this study, we believe the equation may involve four orders with nonlinear viscous terms. That is, one may consider the baroreceptor to be one (first or second order) system inside another, the wall (second order), and the endothelial strain-mediated release of a vasoactive compound to be the nonlinear influence (first-order feedback). Results of this study support this approach, yet, more work is needed to understand mechanotransduction. Andresen and Kunze (48) suggested that a common mechanism may underlie mechanotransduction in various receptor types, even when located in different species, and the difference in receptor-activity responses may be due to "the structure of the tissues in which the receptor endings are embedded." We agree and suggest that the following hypothesis and possibilities need examination. The hypothesis proposes that intrinsic transduction enzyme kinetics are zero order. Intrinsic transduction encodes mass and viscous and elastic influences to produce dynamic activity response. Viscous and elastic influences vary with the type of tissue attached to a baroreceptor. The viscous influence of attached smooth muscle is altered by the presence of vasoactive mediators.

This study was supported in part by University of North Dakota School of Medicine Grant BSRG 2507 RR05 407-29 and American Heart Association, North Dakota Affiliation Grant DA-91-G-01.

1. Dobrin PB. Mechanical properties of arteries. Physiol Rev **58**:397–460, 1978.
2. Kircheim HR. Systemic arterial baroreceptor reflexes. Physiol Rev **56**:100–176, 1976.
3. Mendelowitz D, Scher AM. Pulsatile sinus pressure changes evoke sustained baroreflex responses in awake dogs. Am J Physiol **255**:H673–H678, 1988.
4. Undesser KP, Lynn MP, Bishop VS. Rapid resetting of aortic nerves in conscious rabbits. Am J Physiol **246**:H302–H305, 1984.
5. Dorward PK, Andresen MC, Burke SL, Oliver JR, Korner PI.

Rapid resetting of the aortic baroreceptors in the rabbit and its implications for short-term and longer term reflex control. Circ Res **50**:428–439, 1982.
6. Coleridge HM, Coleridge JG, Kaufman MP, Dangel A. Operational sensitivity and acute resetting of aortic baroreceptors in dogs. Circ Res **48**:676–684, 1981.
7. Coleridge HM, Coleridge JG, Poore ER, Roberts AM, Schultz HD. Aortic wall properties and baroreceptor behavior at normal arterial pressure and in acute hypertensive resetting in dogs. J Physiol **350**:309–326, 1984.
8. Andresen MC, Yang M. Rapid baroreceptor resetting is unaltered by chronic hypertension in rats. Am J Physiol **256**:H1228–H1235, 1989.
9. Heesch CM, Thames MD, Abboud FM. Acute resetting of carotid sinus baroreceptors. I: Dissociation between discharge and wall changes. Am J Physiol **247**:H824–H832, 1984.
10. Munch PA, Andresen MC, Brown AM. Rapid resetting of aortic baroreceptors in vitro. Am J Physiol **244**:H672–H680, 1983.
11. Munch PA, Brown AM. Role of vessel wall in acute resetting of aortic baroreceptors. Am J Physiol **248**:H843–H852, 1985.
12. Salgado H, Krieger EM. Extent of baroreceptor resetting in response to sodium nitroprusside and verapamil. Hypertension **11**:I121–I125, 1988.
13. Chen HI, Chapleau MW, McDowell TS, Abboud FM. Prostaglandins contribute to activation of baroreceptors in rabbits. Circ Res **67**:1394–1404, 1990.
14. Heesch CM, Miller BM, Thames MD, Abboud FM. Effects of calcium channel blockers on the isolated carotid baroreceptors and baroreflex. Am J Physiol **245**:H653–H661, 1983.
15. Brown AM. Receptors under pressure: An update on baroreceptors. Circ Res **46**:1–10, 1981.
16. Brown AM, Saum WR, Yasui S. Baroreceptor dynamics and their relationship to afferent fiber type and hypertension. Circ Res **42**:694–702, 1978.
17. Franz GN, Scher AM, Ito CS. Small signal characteristics of carotid sinus baroreceptors of rabbits. J Appl Physiol **30**:527–535, 1971.
18. Koushanpour E, Kelso DM. Partition of the carotid sinus baroreceptor response in dogs between the mechanical properties of the wall and the receptor elements. Circ Res **31**:831–845, 1972.
19. Aars H. Effects of altered smooth muscle tone on aortic diameter and aortic baroreceptor activity in anesthetized rabbits. Circ Res **28**:254–262, 1971.
20. Rees PM. Observations on the fine structure and distribution of presumptive baroreceptor nerves at the carotid sinus. J Comp Neurol **131**:517–548, 1967.
21. Beachley NH, Harrison HL. Introduction to Dynamic System Analysis. New York: Harper & Row, pp4–200, 1978.
22. Rubanyi GM, Romero JC, Vanhoutte PM. Flow-induced release of endothelium-derived relaxing factor. Am J Physiol **250**: H1145–H1149, 1986.
23. Miller VM. Interactions between neural and endothelial mechanisms in control of vascular tone. News Physiol Sci **6**:60–63, 1991.
24. Stinnett HO, Sepe FJ, Mangusson MR. Rabbit carotid baroreflexes after carotid sympathectomy, vagotomy, and β blockade. Am J Physiol **241**:H600–H605, 1981.
25. Andresen MC, Yang M. Interaction among unitary spike trains: Implications for whole nerve measurements. Am J Physiol **256**:R997–R1004, 1989.
26. Peach MJ, Loeb AL, Singer HA, Saye J. Endothelium-derived vascular relaxing factor. Hypertension **7**(suppl I):I94–I100, 1985.
27. Hartmann A, Saeed M, Bing RJ. Release of endothelium-derived relaxing factor from freshly harvested porcine endothelial cells. Circ Res **61**:548–554, 1987.
28. Ralevic V, Kristek F, Hudlicka O, Burnstock G. A new protocol for removal of the endothelium from the perfused rat hind-limb preparation. Circ Res **64**:1190–1196, 1989.
29. Stinnett HO, Olson MD. Rabbit carotid baroreceptor activity and sinus dimensions before and after protease treatment. Physiologist **29**:34.7, 1986.
30. Stinnett HO, Barman SA, Olson MD. Electron microscope (EM) analysis of nifedipine effect on carotid sinus tissue. Proc Int Un Physiol Sci **16**:P116.20, 1986.
31. Bean BP, Sturek M, Puga A, Hermsmeyer K. Calcium channels in muscle cells isolated from rat mesenteric arteries: Modulation by dihydropyridine drugs. Circ Res **59**:229–235, 1986.
32. Moreland S, Moreland RS. Effects of dihydropyridines on stress, myosin phosphorylation, and V_0 in smooth muscle. Am J Physiol **252**:H1049–H1058, 1987.
33. Kunze DL, Andresen MC, Torres LA. Do calcium antagonists act directly on calcium channels to alter baroreceptor function? J Pharmacol Exp Ther **239**:303–310, 1986.
34. Stinnett HO, Roller CL. Influence of nifedipine levels on rabbit carotid baroreceptor nerve activity. Physiologist **27**:28.3, 1984.
35. Singer HA, Peach MJ. Calcium and endothelial-mediated vascular smooth muscle relaxation in rabbit aorta. Hypertension **4**(suppl II):II-19–II-25, 1982.
36. Barman SA, Saari JT, Olson MD. The effect of verapamil on lanthanum (La^{3+}) binding in the isolated rabbit heart. In: Sperelakis N, Caulfield JB, Eds. Calcium Antagonist. Boston: Martinus Nijhoff, pp257–273, 1984.
37. Fung YC. Biomechanics. New York: Springer-Verlag, pp41–53, 1981.
38. Sokal RR, Rohif FJ. Comparison of regression lines. In: Biometry, 2nd Ed. San Francisco: WH Freeman and Co., pp499–509, 1981.
39. Scarborough JB. Numerical Mathematical Analysis, 6th Ed. Baltimore: Johns Hopkins Press, pp545–547, 1966.
40. Motulsky HJ, Ransnas LA. Fitting curves to data using nonlinear regression: A practical and nonmathematical review. FASEB J **1**:365–374, 1987.
41. Stinnett H, Akers T, Ewert D, Wiggin T. Viscoelastic modeling of carotid sinus baroreceptors. Biomed Sci Inst **25**:13–18, 1989.
42. Stinnett H, Ewert D. Model simulation of baroreceptor resetting. Biomed Sci Inst **26**:185–190, 1990.
43. Srinivasan R, Nudelman HB. Modeling the carotid sinus baroreceptor. Biophys J **12**:1171–1182, 1972.
44. Spickler JW, Kezdi P. Dynamic response characteristics of carotid sinus baroreceptors. Am J Physiol **212**:472–476, 1967.
45. Stinnett HO, Hennes ML. Model inferences on baroreceptor & sinus wall responses. Biomed Sci Inst **27**:105–112, 1991.
46. Stinnett HO, Hennes ML. Model of baroreceptor influenced by mass. FASEB J **5**:A1424, 1991.
47. Andresen MC. Short- and long-term determinants of baroreceptor function in aged normotensive and spontaneously hypertensive rats. Circ Res **54**:750–759, 1984.
48. Andresen MC, Kunze DL. Ionic sensitivity of baroreceptors. Circ Res **61**(suppl I):I-66–I-71, 1987.

Appendix

In this study, wall and baroreceptor multifiber activity responses of the rabbit carotid sinus were used to estimate mechanical properties of the sinus and property influences on baroreceptors as for systems described by linear first- and second-order differential equations (25, 38).

Use of the First-Order Differential. For *analysis*

of wall dimension response (y, in meters), the nonhomogeneous form used was:

$$Cdy/dt + Ky = F \qquad \text{[Eq. 1]}$$

where C = viscosity (N(sec)/m), K = elasticity (N/m), and F = the force (N) proportional to the intrasinus pressure input. System properties were found in solution for y from the transient (y_t) and steady state (y_{ss}) equations, where:

$$y = y_t + y_{ss} \qquad \text{[Eq. 2]}$$

At steady state $dy/dt = 0$, $y = F/K$ and elasticity was:

$$K = F/y \qquad \text{[Eq. 3]}$$

The transient solution required solving the homogeneous equation:

$$(dy/dt) + K/Cy = 0 \qquad \text{[Eq. 4]}$$

Using the principle of superposition, with $p = d/dt$, $x = K/C$, Eq. 6 was rewritten as:

$$y(p + x) = 0 \qquad \text{[Eq. 5]}$$

from which the characteristic equation was:

$$p + x = 0 \qquad \text{[Eq. 6]}$$

The solution for the root (p) was:

$$p = -x = -K/C = -1/\tau \qquad \text{[Eq. 7]}$$

with τ = the system time constant (expansion or contraction, Tables I and II). Root solutions were used in the exponential form of Eq. 4 of the general form:

$$y = A_1 e^{pt} \qquad \text{[Eq. 8]}$$

and specific forms:

$$y = A_1 e^{-(K/C)t} = A_1 e^{-(1/\tau)t} \qquad \text{[Eq. 9]}$$

A_1 is a constant established from initial conditions at $t = 0$. With K and τ determined, the solution for C was:

$$C = K\tau \qquad \text{[Eq. 10]}$$

For *analysis of multifiber activity* response, we considered the wall response (y) as input (see text on transduction-gain), and by substituting (a) for BNA, the nonhomogeneous equation was:

$$Vda/dt + Ea = y \qquad \text{[Eq. 11]}$$

with V = coefficient of viscous-related influence (m(sec)/a) and E = coefficient of elastic-related influence (m/a). E is the reciprocal of the proportional component of transduction-gain and determined from change in steady state activity (Δa_{ss}) and wall dimension (Δy_{ss}). With $da/dt = 0$ and solution of the steady state equation, E was:

$$E = \Delta y_{ss}/\Delta a_{ss} \qquad \text{[Eq. 12]}$$

The transient equation has exponential forms:

$$a = A_2 e^{-(E/V)t} = A_2 e^{-(1/\tau)t} \qquad \text{[Eq. 13]}$$

A_2 is the initial condition constant and τ = the activity time constant for the dynamic component of transduction-gain (decay or recovery, Tables I and II). The viscosity-related influence (V) was estimated from:

$$V = E\tau \qquad \text{[Eq. 14]}$$

Because data consisted of multifiber responses, the time constants of Tables I and II represent averages of a range of time constants involving collective, viscosity-related influences.

Use of the Second-Order Differential. Use of the second-order differential was required considering the sinus as a system with mass (M) and described by the nonhomogeneous equation:

$$M(d^2y/dt^2) + C(dy/dt) + Ky = F \qquad \text{[Eq. 15]}$$

System properties are found in solution for y from transient and steady state equations. At steady state, $d^2y/dt^2 = dy/dt = 0$, $y = F/K$, and elasticity (K) is found from Eq. 3. The transient solution requires solving the homogeneous equation:

$$M(d^2y/dt^2) + C(dy/dt) + Ky = 0 \qquad \text{[Eq. 16]}$$

which has the characteristic equation of:

$$Mp^2 + Cp + K = 0 \qquad \text{[Eq. 17]}$$

with two roots evaluated from:

$$p = [-C \pm (C^2 - 4MK)^{1/2}]/2M \qquad \text{[Eq. 18]}$$

and used in solution of the exponential:

$$y = A_1(e^{-(p1)t}) + A_2(e^{-(p2)t}) \qquad \text{[Eq. 19]}$$

A_1 and A_2 are initial condition constants. The general identity for the sum of roots ($p_1 + p_2$) is:

$$(p_1 + p_2) = -C/M \qquad \text{[Eq. 20]}$$

The identity is not the same as for the first-order differential (Eq. 7). Roots may be equal or unequal and real or complex conjugates. They are best determined with analysis of responses to swept-frequency pressure inputs, which were not done in this study. However, substitution of the estimated coefficient for wall viscosity (C_f) during fast event of the dynamic response, elasticity (K), and mean sinus mass (M) into Eq. 18 suggested that the roots were real and unequal. We also estimated wall damping using a critical viscosity (C_c) calculated from:

$$C_c = 2(MK)^{1/2} \qquad \text{[Eq. 21]}$$

with damping estimated from the ratio (Z):

$$Z = C_f/C_c \qquad \text{[Eq. 22]}$$

In controls, damping increased as viscosity increased due to a feedback influence (see text for estimate of feedback influence characteristics).